MODELLING AND PARAMETER ESTIMATION OF TRANSMISSION LINES

Carlos Frederico Matt
Electric Power Research Center (CEPEL), Avenida Um sem número, Ilha do Fundão, Cidade Universitária, Rio de Janeiro, Brazil, 21944-970
cfmatt@cepel.br

Daniel Alves Castello
Solid Mechanics Laboratory, Mechanical Engineering Department, COPPE/UFRJ, Avenida Um sem número, Ilha do Fundão, Cidade Universitária, Rio de Janeiro, Brazil, 21945-970
castello@mecsol.ufrj.br

Abstract. The present work is aimed at modelling a transmission line conductor as a continuous system with nonuniform bending stiffness and at estimating such a distributed property. The parameter estimation problem has been addressed by the classical Levenberg-Marquardt iterative procedure. Several simulation examples, considering static data, have been performed in order to assess the effectiveness of the estimation. Aiming at obtaining conditions closer to reality, the simulations are performed considering a reduced number of available sensors over the structure and noise-corrupted measurements.

Keywords: transmission line, bending stiffness, parameter estimation, Levenberg-Marquardt

1. Introduction

Wind-excited mechanical vibrations in single conductors of overhead transmission lines are understood as critical problems for the safety and reliability of the transmission line. Different types of mechanical vibrations may occur; however, the most common type corresponds to wind-excited vibrations in the frequency range of 3 Hz to 150 Hz, caused by vortex-shedding (Rawlins, 1979; CIGRE, 1989). The aerodynamic lift forces arising from the periodic shedding of vortices are responsible for the subsequent conductor vibrations. Since the span length of a typical transmission line is of the order of hundred to thousand meters, the frequency spectrum of the conductors is almost continuous. Two consecutive natural frequencies of the conductors are quite close, separated by approximately 0.1 to 0.2 Hz; therefore, the conductors are frequently excited into forced resonant vibrations. Depending on the pattern of the wind flow and on the mechanical damping of the transmission line, the dynamic stresses and strains induced on the constituent wires of the conductors may become dangerously high, especially at the suspension clamps and at the attachment points of Stockbridge dampers. These stresses and strains may lead to fatigue damage on the wires with catastrophic consequences such as the complete rupture of the conductor and interruption on the supply of electric energy. Therefore, needless to say, the understanding of the transmission lines dynamics is a relevant issue. However, since to now, the subject of wind-induced vibrations on transmission line conductors is still open, mainly because little progress has been made into the mathematical modelling of wind excitations and into the energy dissipated by stranded cables, as transmission line conductors, under flexural vibrations, which, in part, can be attributed to little data about the mechanical properties of transmission line conductors, such as the bending stiffness. This work intends to provide more insight into the modelling and estimation of bending stiffness of transmission line conductors by combining mathematical modelling and simulated experimental measurements.

The most common type of conductors of high voltage transmission lines is composed of steel core wires and one to three layers of aluminum wires wound around, commonly referred to as ACSR conductors (Aluminum Conductor Steel Reinforced), as can be seen in Fig. 1. Under operational conditions, these conductors are strung to a specified mechanical load and their ends are clamped at the suspension towers. Due to the complex geometry of a typical ACSR conductor as the one shown in Fig. 1, most of the theoretical models available in the literature considers such a mechanical structure as a continuous system (Claren and Diana, 1969; Dhotarad et al., 1978; Hagedorn, 1982; Hagedorn, 1987; Vecchiarelli et al., 2000; Diana et al., 2000). The most simple models treat the conductors as taut strings while the most sophisticated ones consider them as homogeneous elastic beams with an 'effective' bending stiffness. The taut string model has the disadvantage that no information can be inferred about the stresses and strains induced on the constituent wires of the conductors as a consequence of the wind excitations. Although the elastic beam model seems to be more appropriate to describe the dynamic behavior of such a mechanical structure, there is a great uncertainty about the effective bending stiffness of the conductors, due to the complicated helicoidal geometry of the wires and the forces acting on them during the bending of the conductor.

Papailiou (1997) presented a more sophisticated model to calculate the conductor bending stiffness that takes into account the helicoidal geometry of the wires, the interlayer friction and interlayer slip during bending. The model proposed

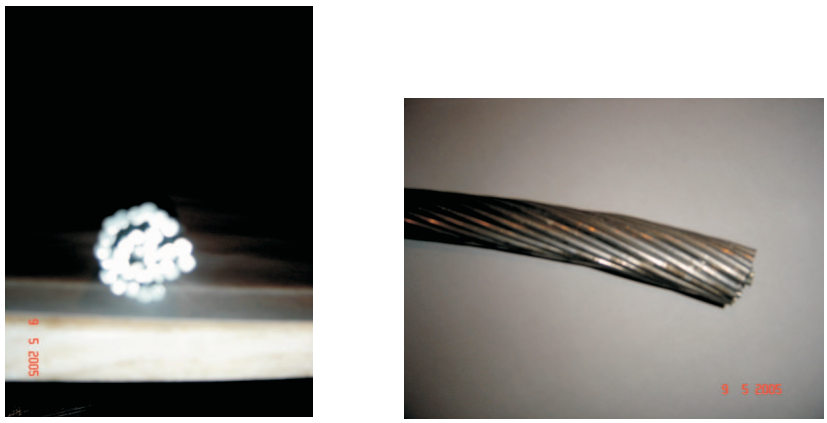

Figure 1. ACSR transmission line conductor with three layers of aluminum wires.

by Papailiou (1997) leads to a variable bending stiffness, i.e., a stiffness which changes with the bending amplitude and the tension applied to the conductor. Nevertheless, in the majority of the works encountered in the literature, the authors adopt a constant bending stiffness for the conductors. The constant value of the bending stiffness is frequently chosen to be within a certain range. The minimum value is obtained by considering the conductor as a bundle of individual wires and by assuming that all wires are free to move relative to each other; thus the minimum value is given by the sum of the bending stiffness of all wires (CIGRÉ, 1979). On the other hand, the maximum value is obtained by also considering the conductor as a bundle of individual wires and assuming that contact pressure among the wires is high enough to prevent their relative motions (CIGRÉ, 1979).

The uncertainty about the bending stiffness of typical conductors comes from the fact that the maximum and minimum bending stiffness values may differ by an order of magnitude. Moreover, experimental measurements performed on laboratory spans indicate that the bending stiffness in the neighborhood of the clamped ends may be much higher, requiring thus a model that accounts for the spatial variation of the bending stiffness. The present work is aimed at modelling the transmission line conductor as a beam with nonuniform bending stiffness and at estimating such a property. Classical inverse analysis techniques such as the Levenberg-Marquardt iterative procedure is used here for the parameter estimation. Several simulation examples, considering static data, have been performed in order to assess the effectiveness of the estimation. Moreover, aiming at obtaining situations closer to reality, it is considered a reduced number of available sensors over the structure and noise-corrupted measurements.

This paper is organized as follows: in section 2, we describe the mathematical formulation of the direct problem and the Levenberg-Marquardt iterative procedure for parameter estimation; in section 3, we present and analyze the results obtained for the bending stiffness based on simulated static data; and, finally, on section 4, we finish by offering the main conclusions of this work and comments about future perspectives.

2. Mathematical formulation of the physical problem

The governing differential equation for the small bending amplitudes $y(x)$ of a transmission line conductor under a general static load $f(x)$, assuming the conductor as an Euler-Bernoulli beam with spatially-variable bending stiffness $EI(x)$, is given by (Claren and Diana, 1969; Dhotarad et al., 1978; Hagedorn, 1987)

$$\frac{\partial^2}{\partial x^2}\left(EI(x)\,\frac{\partial^2 y}{\partial x^2}\right) - T\,\frac{\partial^2 y}{\partial x^2} = f(x), \quad 0 < x < L \tag{1}$$

where x is the spatial coordinate; L is the span length and T is the mechanical load applied to the conductor. Here we suppose that both T and L are constants. In Eq. (1), the distributed bending stiffness was assumed to be given by

$$EI(x) = \begin{cases} EI, & x_c < x < L - x_c \\ \eta\, EI, & x \le x_c \quad \text{and} \quad L - x_c \le x \le L \end{cases} \tag{2}$$

The parameter η appearing on Eq. (2) is the amplification factor of the bending stiffness in the neighborhood of the two ends of the conductor. The frontiers where there is a sudden change in the conductor bending stiffness are given by the positions $x = x_c$ and $x = L - x_c$. Here, we impose the constraint $x_c \le 0.2\,L$. To solve the governing differential equation given by Eq. (1) we must specify the boundary conditions at the ends $x = 0$ and $x = L$. For simple-supported ends, the vertical displacements $y(0)$ and $y(L)$, and the curvatures $y''(0)$ and $y''(L)$ must be zero. For rigidly-clamped ends, the above mentioned vertical displacements and the slopes $y'(0)$ and $y'(L)$ must be zero. Here and in what follows, the prime symbol $(\bullet)'$ stands for differentiation of a function with respect to the space variable x.

2.1 Direct problem

The direct problem comprises the solution of Eq. (1) with appropriate boundary conditions, once η and x_c are known. Here, we solved the direct problem through the classical finite-element method (Reddy, 1993; Hughes, 2000) with Hermite interpolating polynomials for the displacements and slopes. The discretization of the system is such that the global stiffness matrix $\mathbf{K}$ is parameterized as a function of the parameters η and x_c and the direct problem may be formulated as follows

$$\mathbf{K}(\eta, x_c)\bar{\mathbf{y}} = \mathbf{f} \tag{3}$$

where $\bar{\mathbf{y}}$ and $\mathbf{f}$ are, respectively, the vectors containing the degrees of freedom corresponding to the displacement field and static force. The finite element meshes were generated in such a way that the element size in the regions $x \leq x_c$ and $L - x_c \leq x < L$ (henceforth, simple referred to as near-ends region) are always smaller than the element sizes in the region $x_c < x < L - x_c$ (henceforth, simple referred to as far-ends region).

2.2 Inverse problem

For the inverse problem of parameter estimation considered in this work, the amplification factor, η, and the frontier at which there is a sudden change in the conductor bending stiffness, x_c, are regarded as unknowns. The additional information used to estimate these two parameters are the static displacement measurements taken at prescribed locations $x = x_n$, $n = 1, 2, \ldots, N$, along the conductor, where N is the total number of sensors. The problem given by Eq. (1) with $EI(x)$ parameterized according to Eq. (2) is an inverse problem in which the parameters η and x_c are to be estimated. The solution of this inverse problem for the estimation of the above two parameters is based on the minimization of the ordinary least squares norm given by (Özişik and Orlande, 2000)

$$S(\mathbf{P}) = \left[\mathbf{u} - \mathbf{y}(\mathbf{P})\right]^T \left[\mathbf{u} - \mathbf{y}(\mathbf{P})\right]. \tag{4}$$

In Eq. (4), $S(\mathbf{P})$ is the sum of square errors or objective function which is to be minimized; $\mathbf{P}^T$ is the two-column vector of unknown parameters (here, $P_1 = \eta$ and $P_2 = x_c$); $\mathbf{u}$ and $\mathbf{y}(\mathbf{P})$ are, respectively, the vectors of measured and estimated displacements, both evaluated at locations $x = x_n$, $n = 1, 2, \ldots, N$; and the superscript $(\bullet)^T$ denotes the transpose operation. The vector of estimated displacements, $\mathbf{y}(\mathbf{P})$, is obtained from the solution of the direct problem at the measurement location, x_n, $n = 1, 2, \ldots, N$, by using the current estimate for the unknown parameters η and x_c. The minimization of $S(\mathbf{P})$, given by Eq. (4), leads to the following iterative procedure for the vector of unknown parameters $\mathbf{P}$ (Beck and Arnold, 1977)

$$\mathbf{P}^{k+1} = \mathbf{P}^k + \left(\mathbf{J}^T\,\mathbf{J}\right)^{-1}\mathbf{J}^T\left[\mathbf{u} - \mathbf{y}(\mathbf{P}^k)\right]. \tag{5}$$

In Eq. (5), $\mathbf{J}$ denotes the sensitivity or Jacobian matrix given by (Özişik and Orlande , 2000)

$$\mathbf{J}(\mathbf{P}) = \left[\frac{\partial \mathbf{y}^T(\mathbf{P})}{\partial \mathbf{P}}\right]^T = \begin{bmatrix} \frac{\partial y_1}{\partial P_1} & \frac{\partial y_1}{\partial P_2} \\ \frac{\partial y_2}{\partial P_1} & \frac{\partial y_2}{\partial P_2} \\ \vdots & \vdots \\ \frac{\partial y_n}{\partial P_1} & \frac{\partial y_n}{\partial P_2} \end{bmatrix}, \tag{6}$$

with the sensitivity coefficients, J_{ij}, $i = 1, 2, \ldots, n$, $j = 1, 2$, given by the partial derivative of the solution of the direct problem at the measurement location $x = x_i$ with respect to the parameter P_j. Once we obtain the solution of the direct problem using the current estimates for the unknown parameters, we can easily compute the sensitivity matrix.

Frequently, inverse problems of parameter estimation are too ill-conditioning, specially near the initial guess used for the unknown parameters; therefore, $\det \mathbf{J}^T\,\mathbf{J} \approx 0$, causing numerical instabilities in the application of the iterative procedure given by Eq. (5). Hence, we have employed the Levenberg-Marquardt method (Levenberg, 1944; Marquardt, 1963; Beck and Arnold, 1977; Özişik, 1993), which alleviates such difficulties by utilizing the following iterative procedure (Özişik and Orlande, 2000):

$$\mathbf{P}^{k+1} = \mathbf{P}^k + \left(\mathbf{J}^T\,\mathbf{J} + \mu^k\,\mathbf{\Omega}^k\right)^{-1}\mathbf{J}^T\left[\mathbf{u} - \mathbf{y}(\mathbf{P}^k)\right]. \tag{7}$$

The purpose of the matrix term $\mu^k\,\mathbf{\Omega}^k$ is to damp oscillations and instabilities due to the ill-conditioning near the initial guess, by making its components large as compared to those of $\mathbf{J}^T\,\mathbf{J}$, if necessary (Orlande and Özişik, 2000). In this work, we have decided to take the matrix $\mathbf{\Omega}^k$ as the diagonal matrix corresponding to $\mathbf{J}^T\,\mathbf{J}$, following the recommendations of Marquardt (1963). The stopping criteria for our implemented Levenberg-Marquardt iterative procedure were the ones suggested by Dennis and Schnabel (1983), which are $S(\mathbf{P}^{k+1}) < \epsilon_1$, $||\mathbf{J}(\mathbf{P}^{k+1})^T\left[\mathbf{u} - \mathbf{y}(\mathbf{P}^{k+1})\right]||_{L_2} < \epsilon_2$ and $||\mathbf{P}^{k+1} - \mathbf{P}^k||_{L_2} < \epsilon_3$. The symbols ϵ_1, ϵ_2 and ϵ_3 denote user-prescribed tolerances. In this work we set all them to 10^{-9}.

2.3 Sensitivity Matrix

The calculation of the sensitivity matrix **J** is required for the estimation process. In fact, for its computation, it is necessary to obtain the derivatives of the estimated displacements with respect to η and to x_c. The derivative with respect to η can be obtained by means of the differentiation of Eq. (3) as follows

$$\frac{\partial \mathbf{K}}{\partial \eta}\bar{\mathbf{y}} + \mathbf{K}\frac{\partial \bar{\mathbf{y}}}{\partial \eta} = \mathbf{0}. \tag{8}$$

After some mathematical manipulations, Eq. (8) renders as follows

$$\frac{\partial \bar{\mathbf{y}}}{\partial \eta} = -\mathbf{K}^{-1}\frac{\partial \mathbf{K}}{\partial \eta}\bar{\mathbf{y}}. \tag{9}$$

Therefore, the determination of the derivative of $\bar{\mathbf{y}}$ with respect to η is straightforward. Nevertheless, the derivative of $\bar{\mathbf{y}}$ with respect to x_c has to be approximated. In the present work, it will be used the finite differences approach to compute the derivative of the estimated displacement with respect to x_c, viz. :

$$\frac{\partial \bar{\mathbf{y}}}{\partial x_c} = \frac{\bar{\mathbf{y}}(\eta, x_c(1+\lambda)) - \bar{\mathbf{y}}(\eta, x_c)}{\lambda\, x_c} \tag{10}$$

where λ is a prescribed value.

3. Results

Aiming at assessing the effectiveness of the proposed methodology to estimate the parameters, some simulation results will be presented in this section. The values chosen for the dimensions and mechanical properties of the system under consideration for the simulations are typical of transmission line conductors tested on the laboratory span of Electric Power Research Center (CEPEL). Hence, in our simulation results, the cross-section area A, the inertia moment I, the Young's Modulus E and the span length L were chosen to be equal to $7.1 \times 10^{-4}\,\mathrm{m}^2$, $3.98 \times 10^{-8}\,\mathrm{m}^4$, $207\,\mathrm{GPa}$ and $40\,\mathrm{m}$, respectively. The mechanical load T applied to the system was considered to be equal to 2.0×10^4 N.

In order to better understand the estimation process applied to the system under analysis, the authors have decided to consider two estimation problems. The first one considers only the parameter η as being unknown, while the second one considers both the parameters η and x_c as being unknown. Moreover, the assessment of the present approach will consider typical shortcomings such as small number of sensors and noise-corrupted measured information. Measurements containing random errors **u** are simulated by adding an error term to the true response $\mathbf{u}^{exp}$ such as follows:

$$u_j = u_j^{exp} \times (1 + \sigma\,\omega_j) \tag{11}$$

where σ and ω correspond, respectively, to a prescribed value and to a random variable with normal distribution, zero mean and unitary deviation.

In all simulations, the domain $0 < x < L$ was discretized using thirty linear finite elements. Figure 2 shows schematically a typical finite element mesh used in this work, as well as some degrees of freedom related to the nodal vertical displacements. A static force of magnitude 10^3 N was applied at the position $x = 17.6\,\mathrm{m}$. Later on, we will study the effect of the position of the static load on the accuracy of the estimation process. In this work, we estimated the parameters η and x_c for only one type of load: a concentrated one applied at a prescribed finite-element nodal point. In Fig. 2, the nodal point where the force is applied corresponds to the node related to the 27^{th} degree of freedom.

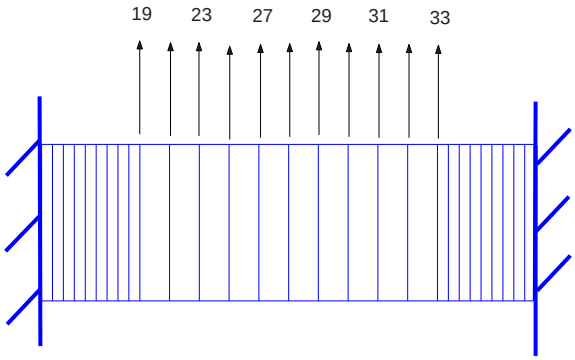

Figure 2. Finite element mesh and some degrees of freedom.

Table 1 shows some estimation results, henceforth denoted by $\hat{\eta}$, for different numbers of sensors, levels of noise and the extension x_c. As it has been considered the measured signals were noise-corrupted, the presented results correspond

Table 1. Results for η estimation.
Average results of 25 runs.

Case	η	η^0	$\hat{\eta}$	$x_c\ (m)$	σ	$DOF\ measured$
1	1000	1	1000	5	0	$21, 23, 25, 27, 29, 31, 33, 35, 37$
2	1000	1	931	5	10^{-2}	$21, 23, 25, 27, 29, 31, 33, 35, 37$
3	1000	1	876	5	2×10^{-2}	$21, 23, 25, 27, 29, 31, 33, 35, 37$
4	1000	1	1000	5	0	$21, 23, 25, 27$
5	1000	1	940	5	10^{-2}	$21, 23, 25, 27$
6	1000	1	866	5	2×10^{-2}	$21, 23, 25, 27$
7	1000	1	1000	3	0	$21, 23, 25, 27$
8	1000	1	840	3	10^{-2}	$21, 23, 25, 27$
9	1000	1	729	3	2×10^{-2}	$21, 23, 25, 27$
10	1000	1	1000	1	0	$21, 23, 25, 27$
11	1000	1	257	1	1×10^{-2}	$21, 23, 25, 27$

to the average of twenty-five runs. >From Table 1, it is clear that, whenever the measured signals were not corrupted with noise, the estimate $\hat{\eta}$ exactly matched the true value η. Another important feature to be emphasized is the fact that, for the system under analysis, as x_c decreases the estimation gets worse. One can probably find an explanation for this behavior based on the concept of sensitivity analysis. It seems reasonable that the effect of the parameter on the measured responses decreases as x_c decreases.

Assuming that the positions of the sensors are held fixed, one can vary the position of the applied load aiming at obtaining more accurate results. Table 2 shows some results considering different positions for the applied force. >From

Table 2. Results for η estimation for different positions of the static load applied.
Average results of 100 runs.

Case	η	η^0	$\hat{\eta}$	$x_c\ (m)$	σ	$DOF\ measured$	$DOF\ force$
12	1000	1	447	1	0	$21, 23, 25, 27$	17
13	1000	1	476	1	10^{-2}	$21, 23, 25, 27$	15
14	1000	1	510	1	10^{-2}	$21, 23, 25, 27$	13
15	1000	1	558	1	10^{-2}	$21, 23, 25, 27$	11
16	1000	1	610	1	10^{-2}	$21, 23, 25, 27$	9
17	1000	1	693	1	10^{-2}	$21, 23, 25, 27$	7
18	1000	1	779	1	10^{-2}	$21, 23, 25, 27$	5
19	1000	1	970	3	2×10^{-2}	$21, 23, 25, 27$	5
20	1000	1	984	5	2×10^{-2}	$21, 23, 25, 27$	5

Case 12 to Case 18 it was considered the extension $x_c = 1\,\mathrm{m}$ which, from Table 1, proved to be the worst cases among the analyzed situations. From the simulation results shown in Table 2, it is clear that, as the applied force position moves towards the end of the beam, the accuracy of estimates is significantly improved. The comparisons between Cases 19 and 9 and between Cases 20 and 6 also show the improvement of the estimated parameters. Therefore, for the next simulations presented in this work, the position where the force is applied will be taken as close as possible to the end $x = 0$ of the beam. One point to be emphasized is that the conditions under which an experiment should be conducted aiming at obtaining more accurate results is defined as optimum experiment design (Beck and Arnold, 1977; Emery and Nenarokomov, 1998). Hence, the best way to choose the positions at which the sensors should be placed, which type of excitation should be used, the time interval that should be measured among others, is to use the concept of optimum experiment design. Based on the optimum experiment design it is possible to maximize the accuracy of the estimates (Emery and Nenarokomov, 1998). The optimum experiment design will be implemented in future investigations when actual measured data on laboratory spans will be supplied to the Levenberg-Marquardt iterative procedure, in order to obtain the estimates for the parameters η and x_c.

As previously mentioned, it was considered that the extension x_c was known for the simulations presented until this point. In order to make the simulation environment closer to a real-like situation, now it will be considered some cases where the extension x_c adopted to generate the estimated displacements $\mathbf{y}$ is different from the one that is used to generate the measured response $\mathbf{u}$. Table 3 shows the results of the simulations for different levels of error in the value adopted for

the extension $x_c = 3\,\mathrm{m}$. For the sake of simplicity, the variation of the extension x_c, δx_c, will be computed as follows

$$\delta x_c = \frac{(x_c^{mod} - x_c)}{x_c} \times 100\% \tag{12}$$

where x_c^{mod} and x_c corresponds, respectively, to the extension adopted in the model and to the actual extension which was used to generate the experimental response $\mathbf{u}$. Table 3 contains some estimation results considering a level of 10% of error in the extension x_c. The results shown in Table 3 presents coherent estimations for the parameter η. Nevertheless, it

Table 3. Results for η estimation considering a level of error in x_c.
Average results of 100 runs.

Case	η	x_c(m)	δx_c(%)	η^0	$\hat{\eta}$	Error in η (%)	σ	$DOF\ measured$	$DOF\ force$
21	1000	5	10	1	1061	6.1	10^{-1}	$21, 23, 25, 27, 29, 31, 33, 35, 37$	3
22	100	5	10	1	98	2	10^{-1}	$21, 23, 25, 27, 29, 31, 33, 35, 37$	3
23	10	5	10	1	9.6	4	10^{-1}	$21, 23, 25, 27, 29, 31, 33, 35, 37$	3

is necessary to extend such an analysis for a broader scenario, including, for example, different values of the extensions x_c and different initial guesses for η. Such an analysis will also be a subject for future investigations.

In the last simulations, both x_c and η are unknowns. For these simulations, it should be emphasized that, whenever the sensitivity matrix has to be calculated, a new finite element mesh must be generated. This change in the finite element mesh is required to obtain, by finite differences, the derivative of the displacement vector $\mathbf{y}$ with respect to the extension x_c. For the sake of simplicity, the authors decided to change the finite element mesh only in the domain Ω_m (far-ends region) defined as follows

$$\Omega_m = [0, x_c] \cup\ [L - x_c, L] \tag{13}$$

The fact that the finite element mesh changes only in Ω_m enables one to assure that the position of the nodes in the domain $(x_c, L - x_c)$ does not vary during the estimation process even though x_c varies.

The variation of the extension x_c is required to calculate the sensitivity matrix $\mathbf{J}$. At this point, one aspect that is relevant was clearly stated by Schnur and Zabaras (1992) and the authors of the present work are going to restate it accordingly to the present problem as follows: The variations of x_c to be used in the finite difference approximation needs to be large enough to be distinguishable in the finite element meshes but small enough to provide accurate finite difference approximations; otherwise, or there will be no update in the parameter x_c into the Levenberg-Marquardt iterative procedure (because the sensitivity coefficients related to such parameter will be closer to zero) or the sensitivity coefficients will not be accurately computed giving thus bad estimates for the parameter x_c. For the simulations presented here it was adopted $\lambda = 10^{-2}$.

Table 4 shows some estimation results when both parameters were regarded as unknowns. The results of Case 24 and Case 25 can be considered accurate for the parameter η and not so accurate for the parameter x_c. The example of Case 26 failed to converge. Schnur and Zabaras (1992) also encountered difficulties in the convergence of Levenberg-Marquardt iterative procedure for their geometric unknown parameter, if the initial guess for such parameter was about $\pm 25\%$ far away from the corresponding correct value, regardless of the simulated measurements were noise-corrupted or not. Here, the geometric parameter analogous to the one of Schnur and Zabaras (1992) is the extension x_c. For the Case 26 of Table 4, the initial guess for the unknown geometric parameter x_c was set to be $+16\%$ far away from the corresponding correct value and even so the Levenberg-Marquardt procedure failed to converge. The authors are still investigating the possible reasons for the bad estimates achieved for both η and x_c in Case 26.

Table 4. Results for η estimation considering an error in x_c.
Average results of 100 runs.

Case	η	η^0	$\hat{\eta}$	x_c (m)	x_c^0 (m)	$\hat{x}_c$ (m)	σ	$DOF\ measured$	$DOF\ force$
24	1000	2000	1096	5	6.25	5.8	10^{-1}	$21, 23, 25, 27, 29, 31, 33, 35, 37$	3
25	1000	1500	1047	5	5.8	5.4	10^{-1}	$21, 23, 25, 27, 29, 31, 33, 35, 37$	5
26	1000	500	691	5	5.8	3.3	10^{-1}	$21, 23, 25, 27, 29, 31, 33, 35, 37$	5

4. Concluding Remarks and Comments on Future Works

In this work, the authors modelled a transmission line conductor as a continuous system with a non uniform bending stiffness and estimated such a distributed property. As a first approach, the bending stiffness was adopted as being piece-wise constant, thus demanding only two parameters, η and x_c, to completely describe it over the system. A finite element model of the structure was built such that the stiffness matrix of the system is parameterized by the unknown parameters η and x_c. The classical Levenberg-Marquadt parameter estimation technique has been used to estimate the unknown parameters of the structure. The sensitivity coefficients associated to the parameter η were computed through the solution of the algebraic system of linear equations resulting from the finite element discretization scheme. The sensitivity coefficients associated to the parameter x_c were computed through classical finite difference formulas. Several simulation examples, considering static data, have been performed in order to assess the effectiveness of the estimation. Aiming at obtaining simulations closer to reality, they were performed considering a reduced number of available sensors over the structure and noise-corrupted measurements. The effects of the number of sensors, point of application of the static load, level of noise of the simulated experimental data and extension x_c on the accuracy of the estimates were analyzed. The authors concluded that an improved accuracy for the estimated parameters was achieved as the point of application of the load approaches the clamped ends of the conductor. The results of this work encourage the implementation of the concept of optimum experiment design which has been proved to be a powerful tool for obtaining accurate parameter estimations. In future investigations, the authors also intend to analytically solve the direct problem with appropriate boundary conditions, in order to overcome the difficulties encountered (and already verified by other authors) for the finite-difference approximation of the sensitivity coefficients related to the unknown geometric parameter x_c.

5. Acknowledgements

The authors would like to gratefully thank Prof. Fernando Alves Rochinha, from Department of Mechanical Engineering at COPPE/UFRJ, and Miss Bianca Walsh, from PUC/RJ, for all their kindly support and fruitfully discussions.

6. References

Beck, J. V. and Arnold, K. J., 1977, "Parameter estimation in engineering and science, Wiley, New York, 501p.

CIGRÉ SC 22 WG 01, 1989, "Report on aeolian vibration", Electra, Vol. 124, pp. 41-77.

Claren, R. and Diana, G., 1969, "Mathematical analysis of transmission line vibration", IEEE Transactions on Power Apparatus and Systems, Vol. 88, No. 12, pp. 1741-1771.

Dennis, J. and Schnabel, R., 1983, "Numerical methods for unconstrained optimization and nonlinear equations, Prentice Hall, Inc., 378p.

Dhotarad, M. S., Ganesan, N. and Rao, B. V. A., 1978, "Transmission line vibrations", Journal of Sound and Vibration, Vol. 60, No. 2, pp. 217-237.

Diana, G., Falco, M., Cigada, A. and Manenti, A., 2000, "On the Measurement of Overhead Transmission Line Conductor Self-Damping", IEEE Transactions on Power Delivery, Vol. 15, No. 1, pp. 285-292.

Emery, A. F. and Nenarokomov, A. V., 1998, "Optimum Experiment Design", Measurement Science Design and Technology, Vol. 9, pp. 864-876.

Hagedorn, P., 1982, "On the computation of damped wind-excited vibrations of overhead transmission lines", Journal of Sound and Vibration, Vol. 83, No. 2, pp. 253-271.

Hagedorn, P., Schmidt, J. and Nascimento, N., 1987, "Stochastic field processes in the mathematical modelling of damped transmission line vibrations", Mathematical Modelling, Vol. 8, pp. 359-363.

Hughes, T. J. R., 2000, "The finite element method - Linear static and dynamic finite element analysis", Dover Publications, Inc., New York, 682p.

Levenberg, K., 1944, "A method for the solution of certain non-linear problems in least squares", Quarterly Applied Mathematics, Vol. 2, pp. 164-168.

Marquardt, D. W., 1963, "An algorithm for least squares estimation of nonlinear parameters", Journal of the Society for Industrial and Applied Mathematics, Vol. 11, pp. 431-441.

Özişik, M. N., 1993, "Heat conduction", John Wiley & Sons, Inc., New York, 692p.

Özişik, M. N. and Orlande, H. R. B. 2000, "Inverse Heat Transfer: Fundamentals and Applications", Taylor & Francis, 160p.

Papailiou, K. O., 1997, "On the bending stiffness of transmission line conductors", IEEE Transactions on Power Delivery", Vol. 12, No. 4, pp. 1576-1588.

Rawlins, C. B., 1979, "Transmission Line Reference Book: Wind-Induced Conductor Motion", Ed. EPRI, Palo Alto, California, 244p.

Reddy, J. N., 1993, "Introduction to the finite element method", McGraw-Hill, 896p.

Schnur, D. S. and Zabaras, N., 1992, "An inverse Method for Determining Elastic Material Properties and a Material

Interface", International Journal for Numerical Methods in Engineering, Vol. 33, pp. 2039-2057.
Vecchiarelli, J., Currie, I. G. and Havard, D. G., 2000, "Computational Analysis of Aeolian Conductor Vibration with a Stockbridge-Type Damper", Journal of Fluids and Structures, Vol. 14, pp. 489-509.

7. Responsibility notice

The author(s) is (are) the only responsible for the printed material included in this paper